Journal of Rubber Research (2024) 27:373–382
https://doi.org/10.1007/s42464-024-00253-7

ORIGINAL PAPER

The Cerato-Platanin gene, *rmcp*, from *Rigidoporus microporus* was stably expressed during infection of *Hevea brasiliensis*

Nor Afiqah Maiden[1,2] · Safiah Atan[1] · Nusaibah Syd Ali[3] · Khairulmazmi Ahmad[2,3] · Mui-Yun Wong[2,3]

Received: 6 February 2024 / Revised: 15 April 2024 / Accepted: 16 April 2024 / Published online: 4 May 2024

Abstract

The rubber tree (*Hevea brasiliensis*) is vulnerable to infections by various fungal pathogens. White root disease infection is one of the most prevalent diseases of rubber in Malaysia. This disease is caused by the fungus *Rigidoporus microporus*. Delayed management of this disease can cause considerable reduction in total tree stand and ultimately decreased land productivity. The utilisation of elicitor proteins to heighten host plant resistance represents a sustainable approach to disease control by reducing the use of chemical fungicides. The cerato-platanin protein family is the most widely reported class of elicitor proteins. This study isolated a member of the cerato-platanin family from *R. microporus* and evaluated its expression during *H. brasiliensis* infection. Total RNA was extracted from the mycelial sample of *R. microporus* followed by cDNA synthesis, isolation and cloning of the cerato-platanin transcript referred to as *rmcp*. In silico characterisation of the obtained sequence was then conducted and the relative expression of the gene was evaluated using RT-qPCR. A transcript of 438 bp encoding 145 amino acids protein, denoted as RmCP, was isolated and cloned. RmCP is composed of a cerato-platanin domain and a predicted N-terminal signal peptide. Phylogenetic analysis grouped RmCP into a cluster together with cerato-platanin proteins originating from basidiomycetes. The expression of *rmcp* gene was consistent throughout the study period and was not significantly different from axenic culture. This suggests the gene to have a fundamental function in the life cycle of *R. microporus*.

Keywords Cerato-platanin · Elicitor · *Rigidoporus microporus* · *Hevea brasiliensis* · Plant immunity · White root disease

Introduction

There are more than 2500 rubber-producing plants, however, *H. brasiliensis* or more commonly known as the rubber tree is the world's sole commercial producer of natural rubber, making it a plant of great economic importance [1, 2]. However, the rubber tree is vulnerable to attacks by fungal pathogens. The basidiomycete *Rigidoporus microporus* is the causal pathogen for white root disease, one of the most prevalent diseases affecting *Hevea brasiliensis*. The white root disease of rubber, if left untreated, causes reduction in latex yield and land productivity [3].

Elicitors are becoming a prime instrument in plant disease control due to their competence in activating or inducing resistance in plants [4]. During the last decade, numerous studies have identified microbe-derived elicitors that induce immune responses in different plant species [5, 6]. The utilisation of elicitors represents a novel strategy in crop protection to reduce disease incidence, reduce the use of chemical pesticides, and improve crop quality. The

✉ Mui-Yun Wong
muiyun@upm.edu.my

Nor Afiqah Maiden
afiqah@lgm.gov.my

Safiah Atan
safiah@lgm.gov.my

Nusaibah Syd Ali
nusaibah@upm.edu.my

Khairulmazmi Ahmad
khairulmazmi@upm.edu.my

1 Production Development Division, Malaysian Rubber Board, 47000, Sungai Buloh, Selangor, Malaysia

2 Institute of Plantation Studies, Universiti Putra Malaysia, 43400 Serdang, Selangor, Malaysia

3 Department of Plant Protection, Faculty of Agriculture, Universiti Putra Malaysia, 43400 Serdang, Selangor, Malaysia

cerato-platanin (CP) family of proteins is one of the most widely reported groups of elicitor proteins.

Cerato-platanin proteins (CPPs) are small cysteine-rich proteins which are mainly composed of 105 to 134 amino acids with four conserved cysteine residues forming two disulfide bridges which confers CPPs extreme stability to high temperature and acidic media [7]. The first member of the CPP family is the phytotoxic cerato-platanin protein, the eponym of the CPP family, isolated from the culture filtrate of *Ceratocystis fimbriata* f. sp. *platani*, the causal agent for canker stain disease of European plane trees [8]. CPPs are able to trigger plant's immune response, hence, considered as microbe-associated molecular patterns (MAMPs) [9, 10]. Numerous studies reported CPPs to play roles in fungal development and/or in host–pathogen interactions [11–13]. The identification of CPPs from *R. microporus* would facilitate the improvement of white root disease management strategy. Therefore, this study was conducted to isolate a CPP-encoding gene from the rubber white root disease pathogen and evaluate the expression profile of the identified gene during *H. brasiliensis*-*R. microporus* interaction.

Materials and methods

Fungal strain and plant material

The fungus *R. microporus* isolate AM was obtained from Integrated Pest and Disease Management (IPDM) Unit, Malaysian Rubber Board (MRB) and maintained on potato dextrose agar (PDA) at 25 °C in the dark.

Seedlings of *H. brasiliensis* clone RRIM 2002 were purchased from Pendang Nursery Sdn. Bhd. (Pendang, Malaysia) and kept in a greenhouse under natural climatic conditions (25–37 °C, 40–96% relative humidity) at the Sungai Buloh Research Station, MRB.

Extraction of total RNA and cDNA synthesis

Mycelial samples of *R. microporus* were ground with liquid nitrogen using mortar and pestle. The powder was then scooped with a sterile spatula into a microcentrifuge tube. Total RNA was extracted using RNeasy Plant Mini Kit (QIAGEN GmbH, Germany) according to manufacturer's instruction. The quantity and quality of the extracted RNA was determined using NanoDrop ND-1000 UV–Vis Spectrophotometer (NanoDrop Technologies, USA) while the integrity was assessed using agarose gel electrophoresis. The agarose gel was then visualised under UV light using Alpha Imager HP system (Alpha Innotech, USA). The purified RNA was stored at − 80 °C.

Simultaneous removal of genomic DNA and reverse transcription were performed using *TransScript*® One-Step gDNA Removal and cDNA Synthesis Supermix (TransGen Biotech, China). All steps were conducted according to the manufacturer's instruction. The synthesised cDNA was stored at − 20 °C.

Isolation and cloning of rmcp

RT-PCR was performed to isolate the full coding sequence for *rmcp*. Transcript sequence of a cerato-platanin protein referred to as *rmcp* was retrieved from Malaysian Rubber Board's in-house *R. microporus* RL19 draft genome. Primers were designed based on the retrieved sequence using PrimerQuest™ online tool. Sequences of all primers used are listed in Table 1. Amplification was carried out in 20 µL reaction volume containing 2 µL cDNA template, 1 µM of each primer and 1X Phusion Flash High-Fidelity PCR Master Mix (Thermo Scientific, USA). The PCR reaction was performed in a thermal cycler C1000™ Thermal Cycler (Bio-Rad, USA) as follows: the samples were initially denatured at 95 °C for 3 min followed by 30 cycles of denaturation at 95 °C for 40 s, annealing at 63.7 °C for 40 s, and extension at 72 °C for one minute. The final extension step was at 72 °C for 7 min after the final cycle. Agarose gel electrophoresis was used to check for the presence of desired amplified PCR products. The PCR product was sent to Apical Scientific Sdn. Bhd. for sequencing.

The full coding sequence of *rmcp* was amplified and inserted into the pEASY®-Blunt3 cloning vector following the instructions of pEASY®-Blunt3 Cloning Kit (TransGen Biotech, China). The constructed plasmid pEASY-Blunt3-*rmcp* was then transformed into *E. coli* Trans1-T1 competent cells. Colony PCR was carried out to screen positive transformants. Single colonies were picked using sterile toothpick, dipped into 10 µL of sterile ultrapure water, vortexed, and 1 µL of the mixture was used as template. M13 promoter forward primer and *rmcp* reverse primer was used to verify that the insert was ligated with the vector in the correct orientation. Amplification was carried out in 25 µL reaction volume containing 0.5 µM of each primer and 1X DreamTaq Green PCR Master Mix (Thermo Scientific, USA). The PCR reaction was performed in a C1000™ thermal cycler (Bio-Rad, USA) as follows: the samples were initially denatured at 94 °C for 10 min followed by 30 cycles of denaturation at 94 °C for 30 s, annealing at 49 °C for 30 s

Table 1 List of primers used in RT-PCR and sequencing

Primer name	Primer sequence (5′–3′)
rmcp-F	ATGTACTTCAAACTCCCCACCA
rmcp-R	TTAGAGACCACAGTGCCAGCT
M13-F	GTAAAACGACGGCCAGT
M13-R	CAGGAAACAGCTATGAC

and extension at 72 °C for 1 min. The final extension step was at 72 °C for 7 min after the final cycle. The presence of desired amplified PCR products was checked using 1.2% agarose gel in 1 × TBE (89 mM Tris base; 89 mM borate; 2 mM Na_2EDTA), run at 70 V for an hour. The agarose gel was then visualised under UV light using Alpha Imager HP system (Alpha Innotech, USA).

Positive transformant was also verified via sequencing. Single transformed colony was grown overnight in LB broth at 37 °C with shaking at 200 rpm. The pEASY-Blunt3-*rmcp* recombinant plasmid was then isolated from the overnight culture using EasyPure® Plasmid MiniPrep Kit (TransGen Biotech, China) according to manufacturer's instructions. Plasmid quality and quantity was assessed using NanoDrop ND-1000 UV–Vis Spectrophotometer (NanoDrop Technologies, USA). Purified recombinant plasmids were then sent for sequencing using M13 forward and reverse primers.

Verified positive transformants were grown in LB broth overnight at 37 °C with shaking at 200 rpm. The overnight culture was mixed with sterile 80% glycerol in a 1:1 ratio and kept in − 80 °C for long-term storage.

In silico analysis of *rmcp*

The obtained sequence was searched against the National Center for Biotechnology Information (NCBI) Conserved Domain Database (CDD) [14, 15] to verify the presence of CP domain. The subcellular localisation and presence of signal peptides and transmembrane domains were predicted using DeepLoc 2.0 tool [16]. Proteins directed towards the extracellular space containing signal peptide and without transmembrane domains were identified as secreted proteins.

The full-length coding sequences of CPPs from various fungal species were downloaded from the NCBI database. The amino acid sequences were aligned using the MUSCLE program in MEGA version X software [17] with default settings followed by construction of phylogenetic tree using the maximum likelihood method with 1000 bootstrap iterations. The tree was exported into the Interactive Tree of Life (iTOL) online tool [18] for visualisation.

Secondary structures were predicted using Multivariate Linear Regression Combination (MLRC) tool in the Network Protein Sequence Analysis (NPS@) web server [19] with default parameters and 3-D structure modelling were performed using the PHYRE2 web portal [20].

In vitro inoculation of *H. brasiliensis* with *R. microporus*

In vitro inoculation of *H. brasiliensis* seedlings with *R. microporus* was conducted to investigate the expression pattern of *rmcp* gene during host–pathogen interaction. Glass cylinder (1.5 L) containing 20 mL of PDA was inoculated with 4 mm mycelial plug from one week old *R. microporus* culture. The cylinders were then plugged with cotton wool and incubated in the dark at room temperature (28 ± 2 °C). After five days, rubber seedlings were removed from polybags and the roots were cleaned with water. The roots were surface sterilised by dipping in 70% ethanol for 30 s and then rinsing three times with sterile distilled water. The seedlings were then placed into the glass cylinders ensuring good contact with the *R. microporus* culture (Fig. 1). The glass cylinders were sealed with cotton wool, covered with aluminium foil, and incubated at room temperature. Mycelia attached to the roots were scraped, placed in aluminium foil, and dipped in liquid nitrogen before storage at − 80 °C. Sample harvesting was performed at 1-, 2-, 3- and 4-weeks post inoculation (wpi). Seven days old pure culture of *R. microporus* was collected as the control sample (0 wpi). Three biological replicates were collected for each treatment at each time point.

Fig. 1 In vitro artificial inoculation of *Hevea brasiliensis* seedling with *Rigidoporus microporus*

Analysis of rmcp expression during *H. brasiliensis-R. microporus* interaction

Calibration curve for all reference genes and gene of interest were plotted to determine PCR amplification efficiency, E (%). Pooled cDNA sample across all treatments and time points was used as template. The cDNA template was diluted through a series of fourfold dilutions covering six dilution points. Sequences of all primers used for RT-qPCR are listed in Table 2. The qPCR reaction was conducted in 15 µL total reaction volume containing 1 µL cDNA template, 0.2 µM of each forward and reverse primer, 1X *TransStart*® Tip Green qPCR SuperMix (TransGen Biotech, China) and nuclease-free water. Each reaction was run with three technical replicates and two no template controls (NTC) were included to monitor cross contamination. Amplification was conducted using CFX96™

Table 2 List of primers used in RT-qPCR of *Rigidoporus microporus*

Primer name	Primer sequence (5′–3′)	Amplicon size (bp)	
		gDNA	cDNA
q*rmcp*-F	GGTCCAAATGGGCTACTTAC	138	138
q*rmcp*-R	CCCTTCGTATGTCAAACTCC		
RmActin-F	TCCTGATGGCCAGGTTAT	246	139
RmActin-R	GTCAAGGTCGCACTTGTAG		
Rmβ-tubulin-F	TATGGGCACCCTCTTGAT	212	127
Rmβ-tubulin-R	GGAGAGAGTTGCGTTGTAAG		
RmeEF1-α-F	TGGTGTGCGTCAACTTATT	180	120
RmeEF1-α-R	GGGTTGTAACCAACCTTCTTA		

Real-Time System (Bio-Rad, USA) with the following cycling parameters: initial denaturation at 94 °C for 30 s followed by 40 cycles of denaturation at 94 °C for 5 s and annealing at 60 °C for 30 s. Melt curve was generated at the end of every reaction from 65 °C to 95 °C with an increment of 0.5 °C for every 5 s to assess amplification specificity. The baseline and quantification cycle (C_q) were determined by CFX Maestro 2.2 software (Bio-Rad, USA). The standard curve of measured C_q value against $\log_{10}$ of relative template concentration (fold dilution) value along with E (%), slope and coefficient of determination (r^2) values was generated using CFX Maestro 2.2 software (Bio-Rad, USA). PCR amplification efficiency was calculated according to the following formula:

$$E(\%) = \left(10^{\frac{-1}{Slope}} - 1\right) \times 100$$

Quantification of *rmcp* gene expression level by RT-qPCR was performed using 1:100 dilution of cDNA as templates. Reference genes *RmActin*, *Rmβ-tubulin* and *RmeEF1-α* were employed as the internal controls. The relative fold change of *rmcp* expression level between treated and control sample was determined according to method described by [21] using CFX Maestro 2.2 software (Bio-Rad, USA).

One-way analysis of variance (ANOVA) was performed to determine significant differences among all time points at significant level (α) equal to 0.05 using CFX Maestro 2.2 software (Bio-Rad, USA). Three biological replicates were measured for each treatment, with three technical replicates conducted for each biological replicate.

Results

The isolation and cloning of *rmcp* full-length coding sequences (CDS)

The RNA extraction from mycelial sample of *R. microporus* yielded 417.09 ng/µL of good quality RNA with $A_{260/280}$ absorbance ratio of 2.2 and $A_{260/230}$ absorbance ratio of 2.5 indicating minimal contamination. The integrity of the sample was also intact as seen via agarose gel electrophoresis. Two distinct RNA bands, the 28S and 18S bands, with 2:1 ratio, were observed with minimal smearing (Fig. 2). The spectrophotometer reading and agarose gel electrophoresis observation confirmed the quality of the extracted RNA to be suitable for subsequent reverse transcription and PCR amplification.

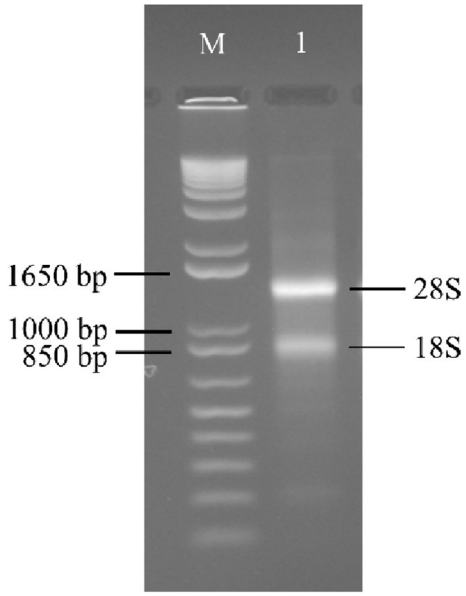

Fig. 2 Total RNA extracted from *Rigidoporus microporus* mycelium. Lane M: 1 Kb Plus DNA Ladder (Invitrogen, USA); Lane 1: *Rigidoporus microporus* total RNA

Five µg of total RNA was used in reverse transcription. Reverse transcription PCR (RT-PCR) using proofreading polymerase was conducted to isolate the full coding region of *rmcp*. The amplification of *rmcp* resulted in band of approximately 400 bp (Fig. 3).

The PCR product was sent for sequencing and the obtained forward and reverse sequences were aligned and merged resulting in a fragment sized 438 bp (GenBank accession: OR880706). The PCR product from amplification of *rmcp* was cloned into the pEASY-Blunt3 expression vector and subsequently transformed into *E. coli* Trans1-T1 competent cells. The transformed cells were screened for positive transformants using colony PCR with M13 forward primer and *rmcp* reverse primer to verify the correct orientation of insert. The analysis of the amplified product revealed band between 500 and 600 bp which was consistent with the expected band size for *rmcp* construct with the correct orientation, 550 bp (Fig. 4).

Additionally, verification of positive transformants with the correct orientation were also conducted via sequencing. Positive transformant identified using colony PCR was

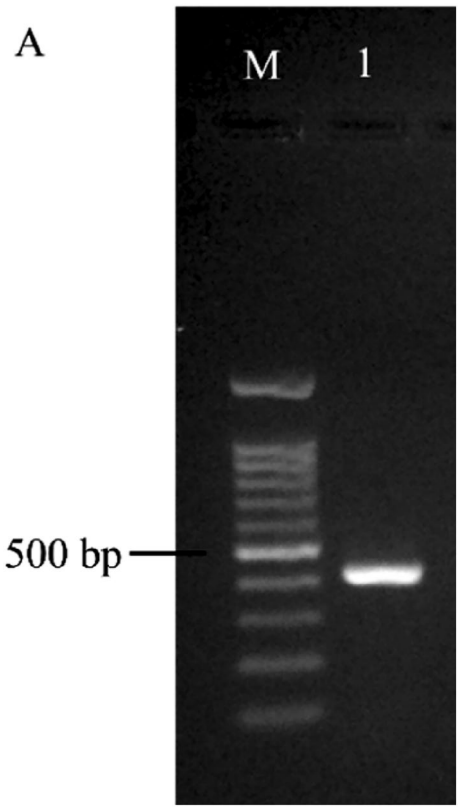

Fig. 3 RT-PCR of full coding sequence of *rmcp*. Lane M: Excel-Band™ 100 bp DNA ladder (SMOBIO Technology, Inc, China), Lane 1: PCR product from amplification of *rmcp*

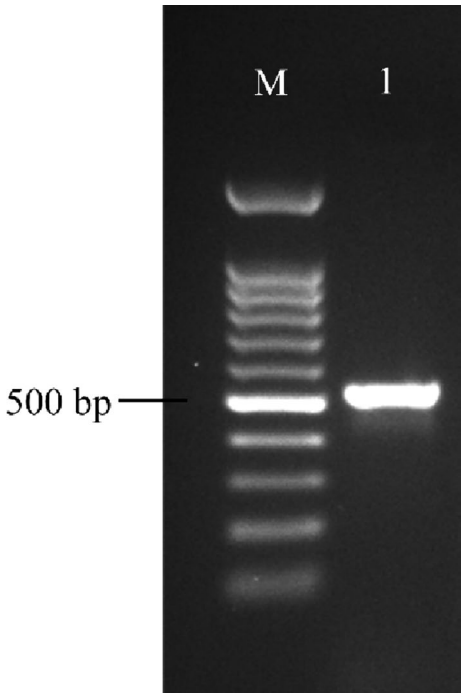

Fig. 4 Colony PCR of transformed competent cells. Lane M: Excel-Band™ 100 bp DNA ladder (SMOBIO Technology, Inc, China), Lane 1: PCR product from amplification of single colony carrying the pEASY®-Blunt3-*rmcp* construct using M13 forward primer and *rmcp* reverse primer

cultured and the plasmid was purified and sent for sequencing using M13 primer pair. The obtained sequences were analysed, and the construct was confirmed to possess the desired insert with the correct orientation.

Sequence analysis of *rmcp*

The *rmcp* gene encodes a protein with 145 amino acid residues. The translated protein, referred to henceforth as RmCP, possess the cerato-platanin domain (29–145 a.a.) with four conserved cysteine residues and a predicted N-terminal signal peptide (1–20 a.a.) (Fig. 5).

Phylogenetic analysis was conducted using the amino acid sequences of RmCP and other experimentally studied members of CPP family. The CPPs were clustered into five groups, Group A, B, C, D, and E (Fig. 6). Group A and E consisted exclusively of CPPs from ascomycetes while Group D is entirely made up of CPPs from basidiomycetes. Group B and C contained a mixture of CPPs from ascomycetes and basidiomycetes. RmCP was clustered into Group D with CPPs from *Moniliopthora perniciosa* and *Heterobasidion annosum*.

The secondary structure prediction using MLRC program revealed RmCP to contain 20.00% α helix, 24.14% extended strand and 55.86% random coil. Protein homology modelling based on a single highest scoring template was employed to predict the 3-D structure of RmCP. The best selected template for RmCP was Sm1 protein from *Trichoderma virens* (PDB entry: 3M3G) with 62% sequence identity. RmCP was modelled with 100% confidence and 82% coverage (Fig. 7). The 3-D models revealed the presence of four α-helices and eight β-strands.

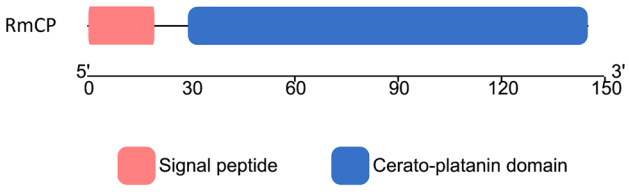

Fig. 5 Features of RmCP sequence as confirmed via CDD search and DeepLoc 2.0 tool. The domains are shown in proportion to the length of the sequence

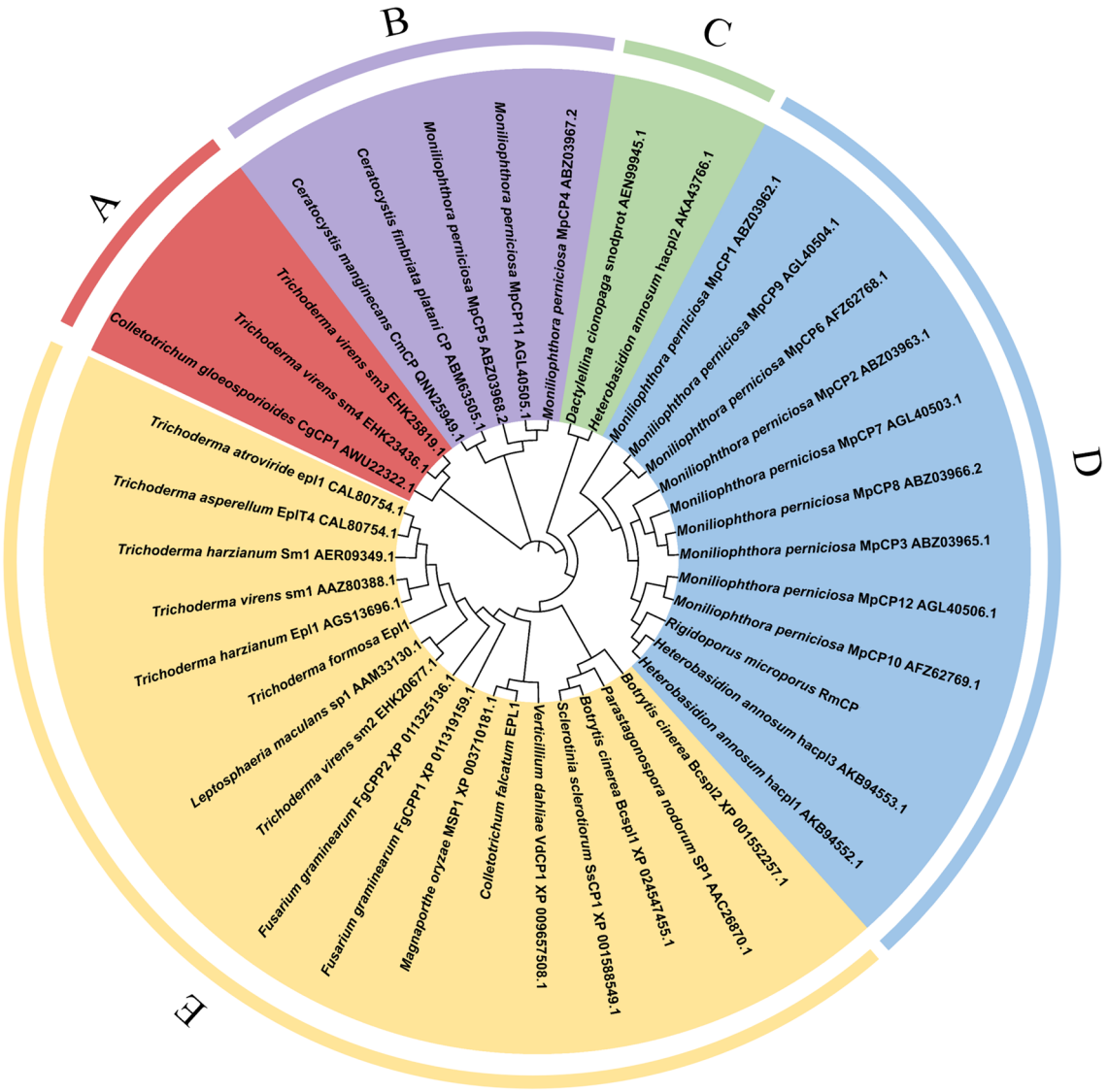

Fig. 6 Phylogenetic relationships among RmCP and CPPs from other fungal species. The phylogenetic tree was constructed using full-length amino acid coding sequences using maximum-likelihood method with 1000 bootstraps in MEGA version X. Different colours indicate different groups. The CPPs were clustered into five groups, Group A (red), Group B (purple), Group C (green), Group D (blue), and Group E (yellow)

Preparation of RT-qPCR template

Total RNA was extracted from mycelium of *R. microporus* at 0, 1-, 2-, 3- and 4-wpi. The RNA concentration as well as purity of the extracted total RNA is listed in Table 3. The absorbance ratio of $A_{260/280}$ and $A_{260/230}$ were between the range of 2.16 to 2.25 and 1.83 to 2.53 respectively, indicating that the RNA samples were of good purity with minimal contamination from protein and organic compounds.

The integrity of the total RNA was evaluated using agarose gel electrophoresis. Two distinct bands of 28S and 18S rRNA were observed with 28S/18S ratio of approximately 2:1 and minimal smearing indicating intact RNA samples with negligible degradation. Additionally, there was no high MW band of genomic DNA signifying absence of genomic DNA contamination (Fig. 8).

rmcp gene expression analysis

Prior to the determination of gene expression level of *rmcp* gene, the PCR amplification efficiency for all primer pairs were evaluated. Additionally, the melt curve step was also included to identify non-specific amplification. The amplification efficiency of all primer pairs ranged from 94.3 to 105.0% while the R^2 ranged from 0.992 to 0.995 indicating a good fit of the regression line.

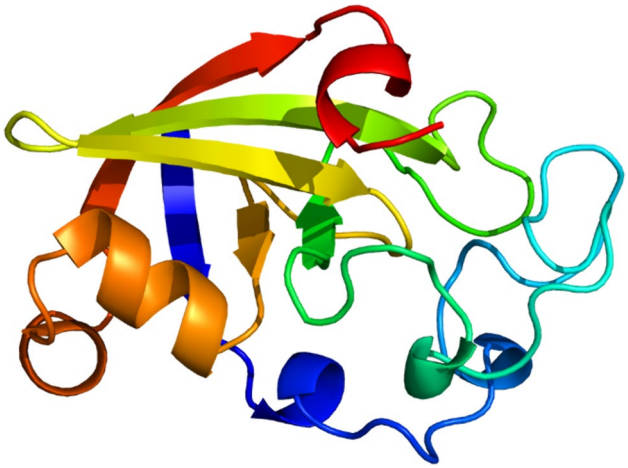

Fig. 7 3-D model of RmCP containing four α-helices and eight β-strands. The model was based on Sm1 protein from *Trichoderma virens* (PDB entry: 3M3G)

Table 3 Yield and purity of total RNA extracted from mycelial samples of *Rigidoporus microporus*

Sample		RNA concentration (ng/μL)	A260/280	A260/230
Time point (weeks post inoculation)	Rep			
0 wpi	1	1601.82	2.24	2.51
	2	1509.33	2.24	2.50
	3	1729.28	2.23	2.45
1 wpi	1	1623.71	2.25	2.51
	2	2951.36	2.16	2.39
	3	3094.31	2.16	2.27
2 wpi	1	1750.03	2.25	1.83
	2	1418.75	2.25	2.49
	3	1468.99	2.24	2.53
3 wpi	1	2116.79	2.21	2.52
	2	1644.21	2.22	2.49
	3	2563.13	2.19	2.49
4 wpi	1	2460.90	2.19	2.48
	2	1811.67	2.23	2.49
	3	2390.22	2.20	2.48

The expression of *rmcp* was normalised against three reference genes, *RmActin*, *Rmβ-tubulin* and *RmeEF1-α*. The expression of *rmcp* at 1, 2, 3, and 4 wpi were calculated relative to the expression of in vitro culturing hypha (0 wpi) as the control. The expression of *rmcp* appeared stable throughout the study period (Fig. 9). Only a slight up-regulation in relative expression level was observed at 1, 2 and 3 wpi with 1.43, 1.22 and 1.36 relative fold change, respectively. The relative expression level at 4 wpi dropped to almost the same as 0 wpi with only 1.02 relative fold change. There was no significant differences in expression across all time points.

Discussion

A transcript belonging to the CPP family was isolated from the rubber fungal pathogen, *R. microporus* and referred to as *rmcp*. The full coding sequence was 438 bp and encodes a protein with 145 amino acid residues. The sequence analysis indicated *rmcp* to be comparable with the typical member of the CP family. Most homologs of CPP have protein lengths from 105 to 241 amino acids and possessed four cysteine residues as well a signature sequence of either CSD or CSN [22]. The RmCP protein is composed of 145 amino acids and contained the four conserved cysteine residues as well as CSD signature sequence. The four cysteine residues form two intramolecular disulphide bridges. The reduction and derivatisation of the disulphide bridges resulted in the loss of solubility and eliciting ability implying their significance in protein stability and function [23]. RmCP also contained N-terminal signal peptide and lacked transmembrane domains. Prediction of subcellular localisation found RmCP to be directed towards the extracellular space. This finding is consistent with numerous reports of members of the CP family being secreted proteins and abundantly found in the secretome [9].

The full coding sequence of RmCP was aligned with other experimentally studied CPPs obtained from published literatures for the construction of phylogenetic tree. Functionally studied sequences were added for comparison and to aid interpretation of the results. The CPPs were clustered into five groups. RmCP was clustered together with CPPs originating from basidiomycetes in Group D. RmCP was found to be most closely related to HaCPL1 and HaCPL3 from *Heterobasidion annosum*. *H. annosum* is the causal pathogen for root and butt rot disease in conifers. Similar to *R. microporus*, this fungus can live as a saprotroph or a necrotroph depending on substrate availability [24]. The structural models of RmCP based on homology modelling showed the presence of four α-helices and eight β-strands. Similar findings were reported for SsCP1 from *S. sclerotiorum*, FocCP1 from *F. oxysporum*, Sm1 from *T. virens* and MpCP1,2,3 and 5 from *M. perniciosa* which had between three and seven α-helices and from six to eight β-strands [11, 25, 26]. The various in silico characterisation performed revealed high similarities between the identified RmCP and previously reported members of the CP family, hence, confirming the identity of RmCP as members of the CP family and further suggesting functional analogy.

The expression of *rmcp* during *H. brasiliensis* and *R. microporus* interaction was investigated to postulate its role. The expression of *rmcp* appeared to be stable throughout

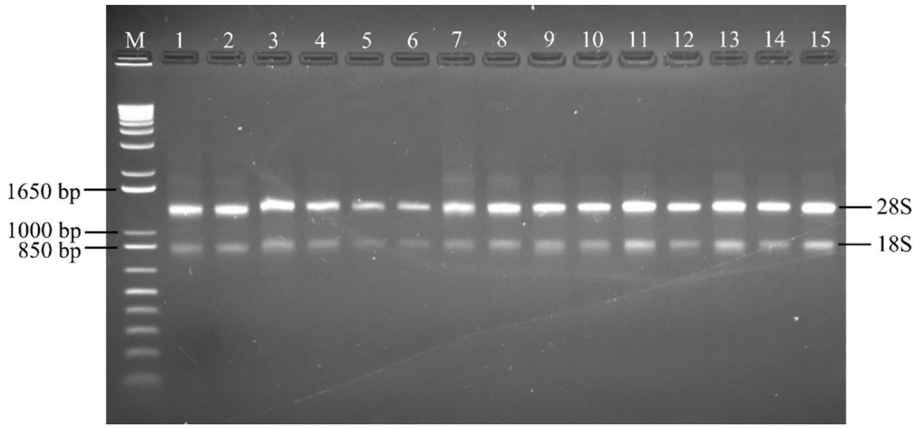

Fig. 8 Total RNA extracted from *Rigidoporus microporus*. Lane M: 1 kb DNA ladder (Invitrogen, USA), Lane 1–3: 0 wpi, Lane 4–6: 1 wpi, Lane 7–9: 2 wpi, Lane 10–12: 3 wpi, Lane 13–15: 4 wpi

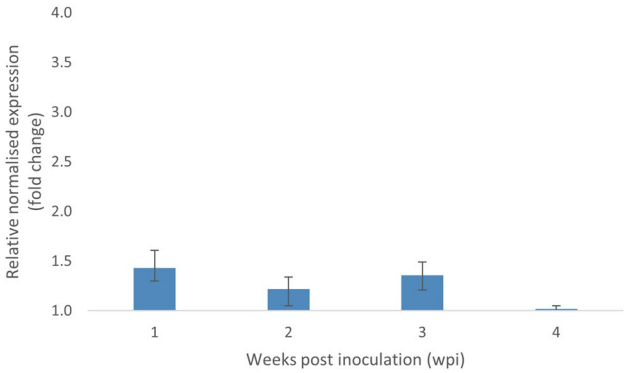

Fig. 9 Relative abundance of *rmcp* transcript during interaction with *Hevea brasiliensis*. The *RmActin*, *Rmβ-tubulin* and *RmeEF1-α* were used as internal control to normalize the data. The relative transcriptional abundance of *rmcp* was determined during infection process at four time points (1-, 2-, 3-, and 4-weeks post inoculation (wpi)) and compared to in vitro culture. Error bars were calculated based on three replicates

sampling time and only a slight up-regulation was observed following interaction with host. This finding was similar to results from the study of CPPs from *H. annosum* [24]. This study identified three *CP* homologues, *hacpl1*, *hacpl2* and *hacpl3*. Based on phylogenetic analysis RmCP was closely related to HaCPL1 and HaCPL3. The expressions of *hacpl1* and *hacpl3* during necrotrophic stage were not significantly different from control as observed in *rmcp*. On the contrary, the expression of *hacpl2* was significantly induced during necrotrophic growth.

Furthermore, other studies on the expression of CP genes during host–pathogen interactions have also reported on the up-regulation of the studied genes following inoculation of host indicating role in plant infection. The expression of *Sscp1* of *Sclerotinia sclerotiorum* was up-regulated more than eight-fold at 12 hpi (hours post inoculation) and maintained up to 48 hpi [11]. The *Fusarium graminearum fgcpp2* gene was also induced as early as 24 hpi and continued to increase up to 72 hpi. The expression of *vdcp1* from *Verticillium dahliae* was reported to continuously increase up to 240 hpi [27]. Although steady expression of *rmcp* was observed in this study, it is important to note that this investigation is limited to after 1 wpi, and the pattern of *rmcp* expression at earlier stages of interaction remains unknown.

The stable expression of *rmcp* in in vitro culture as well as during infection implies a fundamental role in fungal growth and development. This inference is supported by several studies which reported CPP to play a role in fungal growth. The CPP from *Ceratocystis manginecans*, cmcp, was found to be involved in growth of *C. manginecans* besides functioning as a major pathogenicity factor [13]. SsSm1, a CPP from *Sclerotinia sclerotiorum*, was also reported to be involved in hyphal development in addition to role in pathogenicity [28]. Similarly, CgCP1 from *Colletotrichum gloeosporioides* was found to be involved in conidiation and pathogenicity [12]. The multiple roles of CPPs from these reports indicate the possibility of the involvement of RmCP in pathogenicity as well. However, this would need to be empirically verified.

Conclusion

This study identified a member of the CPP family from the rubber white root disease pathogen, *R. microporus*. Full length coding sequence of RmCP was isolated. A sequence of 438 bp encoding 145 amino acids was obtained. Sequence analysis of *rmcp* revealed substantial homogy with other reported members of CPP family. The expression of *rmcp* during interaction between *H. brasiliensis* and *R. microporus* was found to be stable and was not significantly different from axenic culture. This finding suggests a fundamental role in the life cycle of the pathogen. Further studies on *rmcp* would be valuable in elucidating the diverse roles of CPPs in *R. microporus*. The isolation of other homologues of cerato-platanin genes

in *R. microporus* would also be beneficial as basidiomycetes have been reported to hold up to twelve CP-encoding genes suggesting varied and specialised roles of the multiple homologues during fungal life cycle.

Acknowledgements The authors would like to thank the Malaysian Rubber Board for providing equipment, facilities, additional materials, and technical expertise for this study. The authors would also like to thank the Department of Plant Protection, Faculty of Agriculture, Universiti Putra Malaysia for providing real-time PCR system. Special appreciation to Dr. E. Sunderasan for his critical review of the manuscript.

Funding This research was funded by Putra IPB research grant (Grant No. GP-IPB/2017/9523500), Universiti Putra Malaysia.

Data availability Sequence of *rmcp* deposited in NCBI GenBank (GenBank accession: OR880706).

Declarations

Conflict of interest The authors have no conflicts of interest to declare that are relevant to the content of this article.

References

1. Yamashita S, Takahashi S (2020) Molecular mechanisms of natural rubber biosynthesis. Annu Rev Biochem 89:821–851
2. Amerik AY, Martirosyan YT, Martirosyan LY et al (2021) Molecular genetic analysis of natural rubber biosynthesis. Russ J Plant Physiol 68:31–45
3. Mohmad Mahyudin M, Atan S, Ahmad Zambri AM, Noran AS (2022) Tatacara Pengendalian Piawaian Pengurusan Penyakit Akar Putih Di Malaysia, Edisi Pert. Lembaga Getah Malaysia, Kuala Lumpur
4. Hamid S, Wong M-Y (2017) Elicitors and their roles in plant defence against pathogens particularly basidiomycetes. Crop Improv. https://doi.org/10.1007/978-3-319-65079-1_14
5. Li X, Liu M, Liu Y et al (2022) A putative effector of the rubber-tree powdery mildew fungus has elicitor activity that can trigger plant immunity. Planta 255:1–13. https://doi.org/10.1007/s00425-021-03818-7
6. De Britto S, Jogaiah S (2022) Priming with fungal elicitor elicits early signaling defense against leaf spot of broccoli underlying cellular, biochemical and gene expression. Microbiol Res 263:127143. https://doi.org/10.1016/J.MICRES.2022.127143
7. Luti S, Sella L, Quarantin A et al (2020) Twenty years of research on cerato-platanin family proteins: clues, conclusions, and unsolved issues. Fungal Biol Rev 34:13–24. https://doi.org/10.1016/j.fbr.2019.10.001
8. Pazzagli L, Cappugi G, Manao G et al (1999) Purification, characterization, and amino acid sequence of cerato- platanin, a new phytotoxic protein from *Ceratocystis fimbriata* f. sp. platani. J Biol Chem 274:24959–24964. https://doi.org/10.1074/jbc.274.35.24959
9. Pazzagli L, Seidl-Seiboth V, Barsottini M et al (2014) Cerato-platanins: Elicitors and effectors. Plant Sci 228:79–87. https://doi.org/10.1016/j.plantsci.2014.02.009
10. Gaderer R, Bonazza K, Seidl-Seiboth V (2014) Cerato-platanins: a fungal protein family with intriguing properties and application potential. Appl Microbiol Biotechnol
11. Yang G, Tang L, Gong Y et al (2018) A cerato-platanin protein SsCP1 targets plant PR1 and contributes to virulence of *Sclerotinia sclerotiorum*. New Phytol 217:739–755. https://doi.org/10.1111/nph.14842
12. Wang W, An B, Feng L et al (2018) A Colletotrichum gloeosporioides cerato-platanin protein, CgCP1, contributes to conidiation and plays roles in the interaction with rubber tree. Can J Microbiol 64:826–834. https://doi.org/10.1139/cjm-2018-0087
13. Zhang Z, Li Y, Luo L et al (2020) Characterization of cmcp gene as a pathogenicity factor of *Ceratocystis manginecans*. Front Microbiol 11:1–11. https://doi.org/10.3389/fmicb.2020.01824
14. Lu S, Wang J, Chitsaz F et al (2020) CDD/SPARCLE: the conserved domain database in 2020. Nucleic Acids Res 48:D265. https://doi.org/10.1093/NAR/GKZ991
15. Marchler-Bauer A, Bryant SH (2004) CD-search: protein domain annotations on the fly. Nucleic Acids Res 32:W327. https://doi.org/10.1093/NAR/GKH454
16. Thumuluri V, Almagro Armenteros JJ, Johansen AR et al (2022) DeepLoc 2.0: multi-label subcellular localization prediction using protein language models. Nucleic Acids Res 50:W228–W234. https://doi.org/10.1093/NAR/GKAC278
17. Kumar S, Stecher G, Li M et al (2018) MEGA X: molecular evolutionary genetics analysis across computing platforms. Mol Biol Evol 35:1547–1549. https://doi.org/10.1093/MOLBEV/MSY096
18. Letunic I, Bork P (2021) Interactive Tree Of Life (iTOL) v5: an online tool for phylogenetic tree display and annotation. Nucleic Acids Res 49:W293–W296. https://doi.org/10.1093/NAR/GKAB301
19. Combet C, Blanchet C, Geourjon C, Deléage G (2000) NPS@: Network protein sequence analysis. Trends Biochem Sci 25:147–150. https://doi.org/10.1016/S0968-0004(99)01540-6
20. Kelley LA, Mezulis S, Yates CM et al (2015) (2015) The Phyre2 web portal for protein modeling, prediction and analysis. Nat Protoc 106(10):845–858. https://doi.org/10.1038/nprot.2015.053
21. Vandesompele J, De Preter K, Pattyn F et al (2002) Accurate normalization of real-time quantitative RT-PCR data by geometric averaging of multiple internal control genes. Genome Biol 3(research0034):1. https://doi.org/10.1186/GB-2002-3-7-RESEARCH0034
22. Chen H, Kovalchuk A, Keriö S, Asiegbu FO (2013) Distribution and bioinformatic analysis of the cerato-platanin protein family in Dikarya. Mycologia 105:1479–1488. https://doi.org/10.3852/13-115
23. Pazzagli L, Pantera B, Carresi L et al (2006) Cerato-platanin, the first member of a new fungal protein family: cloning, expression, and characterization. Cell Biochem Biophys 44:512–521. https://doi.org/10.1385/CBB:44:3:512
24. Chen H, Quintana J, Kovalchuk A et al (2015) A cerato-platanin-like protein HaCPL2 from *Heterobasidion annosum* sensu stricto induces cell death in *Nicotiana tabacum* and *Pinus sylvestris*. Fungal Genet Biol 84:41–51. https://doi.org/10.1016/j.fgb.2015.09.007
25. Li S, Dong Y, Li L et al (2019) The novel cerato-platanin-like protein FocCP1 from *Fusarium oxysporum* triggers an immune response in plants. Int J Mol Sci 20:1–19. https://doi.org/10.3390/ijms20112849
26. De O, Barsottini MR, De Oliveira JF, Adamoski D et al (2013) Functional diversification of cerato-platanins in moniliophthora perniciosa as seen by differential expression and protein function specialization. Mol Plant-Microbe Interact 26:1281–1293. https://doi.org/10.1094/MPMI-05-13-0148-R
27. Zhang Y, Gao Y, Liang Y et al (2017) The verticillium dahliae snodprot1-like protein VdCP1 contributes to virulence and triggers the plant immune system. Front Plant Sci 8:1–13. https://doi.org/10.3389/fpls.2017.01880

28. Pan Y, Wei J, Yao C et al (2018) SsSm1, a Cerato-platanin family protein, is involved in the hyphal development and pathogenic process of *Sclerotinia sclerotiorum*. Plant Sci 270:37–46. https://doi.org/10.1016/j.plantsci.2018.02.001